Pergamon

Int. J. Heat Mass Transfer. Vol. 39, No. 12, pp. 2409–2426, 1996

0017-9310/96 $15.00 + 0.00

0017-9310(95)00345-2

Dynamics of vapour bubbles in nucleate boiling

YU. A. BUYEVICH and B. W. WEBBON·
NASA Ames Research Center, Moffett Field, CA 94035, U.S.A.

(*Received* 25 *May* 1995 *and in final form* 12 *September* 1995)

Abstract—This paper considers the behaviour of a vapour bubble formed at a nucleation site on a heated horizontal wall. This bubble is modeled as a spherical segment which is separated from the wall by a microlayer of intervening liquid. The liquid is presumed to be at rest at great distances from the bubble. In order to avoid unwarranted assumptions about forces acting on the bubble which are specific to all known models of bubble growth and detachment, we derive equations that govern bubble behaviour in a rigorous way from the variational equation that describes mechanical energy conservation for the whole system, which includes both the bubble and the liquid. The variational equation leads to a set of two mutually independent strongly nonlinear equations which govern bubble expansion and the motion of its centre of mass. Because these equations contain an extra unknown variable (the bubble vapour pressure), a supplementary equation that defines bubble vapour temperature must be formulated with allowance made for heat transfer to the bubble both from the bulk of the surrounding liquid and through the microlayer. The most important conclusion of this paper consists in the fact that surface tension effects result in an effective force that tends to transform the bubble into a sphere, thereby facilitating bubble detachment. This conclusion absolutely nullifies the generally, however erroneously, held belief that this effective force presses the bubble to the wall. By way of example, we consider the evolution of bubbles whose growth is thermally controlled. Our analysis provides quite a natural explanation for a number of repeatedly observed phenomena, such as the influence of gravity and surface tension on bubble growth rate and the dependence of bubble detachment size on thermophysical parameters. Copyright © 1996 Elsevier Science Ltd.

1. INTRODUCTION

Nucleate pool and forced convection boiling are two techniques that are important for the cooling of hot surfaces because relatively small temperature differences result in high heat transfer rates. These techniques can not be effectively applied to diverse industrial and technological problems that require removal of large amounts of generated heat due to a considerable lack of knowledge with respect to the underlying fundamental mechanisms that govern heat transfer properties during boiling processes.

It is clear to any knowledgeable expert in the field that key properties of boiling heat transfer are dictated by the characteristics of vapour bubbles that depart from a superheated surface. In order to determine bubble detachment characteristics, a formidable thermohydrodynamic problem must be solved. On the one hand, vapour bubble evolution involves complicated liquid and vapour flow against an unknown interface, that is, against unknown bubble shape which can be found only in the course of solving the problem. On the other hand, this flow is greatly influenced by (1) the rate of heat transfer in the bulk of liquid near the bubble, (2) the rate of heat transfer through the microlayer separating the bubble from the surface and (3) the rate of vaporization at the interface. Heat transfer is, in its turn, strongly affected by conditions and properties of the flow. This nonlinear feedback between hydrodynamic and thermal phenomena makes the resulting problem practically intractable without drastic model simplifications.

Admittedly, and for this reason, theoretical works on vapour bubble dynamics the present authors are aware of employ more or less plausible postulates concerning forces that act on a bubble as it evolves while attached to a superheated surface and which eventually detaches itself from this surface. It will later be clear that all such postulates are intrinsically wrong with respect to the expected form of the force due to surface tension effects. Quite naturally, mistakes made while studying vapour bubble evolution and while determining both bubble growth rate and bubble detachment size have far-reaching consequences. These mistakes negatively affect conclusions about heat transfer in nucleate boiling in general, and in particular, they cause certain inaccuracies in resultant formulae for heat removal rates.

With a mind to saving journal space, and under the presumption that our reader is adequately acquainted with the appropriate literature, we are not commenting on the accessible information about vapour bubble evolution in detail. But we feel that we must spend some time on the main deficiencies specific to available formulae describing the two most important bubble characteristics: (1) bubble growth rate, and (2) bubble detachment size. There is extensive literature on both these characteristics that is reviewed in a great many papers, manuals and textbooks. As regards bubble growth rate, the state of the art has

NOMENCLATURE

A coefficients defined in equation (2)
a 16/11
C bubble growth constant
E_1, E_2 constituents of kinetic energy
g gravity acceleration
h, H microlayer thickness and corresponding coefficient, equation (20)
K, k coefficients introduced when defining kinetic energy
L latent heat of evaporation
L_s, L_t length and time scales
N_g g/g_e
N_b, N_m, N_σ dimensionless criteria, equations (31), (24) and (36), respectively
p pressure
R bubble radius
S total area of bubble surface
s coordinate of centre of curvature
T temperature
U_c, U_g, U_σ constituents of potential energy
u averaged liquid velocity in microlayer
V bubble volume
w velocity
z coordinate of bubble centre of mass, normal coordinate in microlayer
Ja, Pr Jakob and Prandtl criteria, respectively.

Greek symbols
α, β variables introduced in equations (19)
γ parameter introduced in equation (13)
ΔT $T_w - T_s$
ζ, ξ dimensionless coordinate of centre of curvature and bubble radius
η dimensionless normal coordinate in microlayer
θ angle determining spherical segment shape, Fig. 1(a)
κ ρ_v/ρ_l
λ liquid heat conductivity
ν, ν_e liquid kinematic viscosity and effective ν defined in equation (20)
ρ density
σ surface tension coefficient
τ dimensionless time
χ liquid thermal diffusivity.

Subscripts
d detachment
e Earth conditions
l liquid
s saturation
v vapour
w wall
∞ far from bubble.

not changed much from 1970 when paper [1] was published. No matter whether bubble growth is thermally or inertially controlled, the resultant formulae do not involve the parameters that determine both the buoyancy and surface tension force that are experienced by the growing bubble. (For instance, the well-known parabolic law for thermally controlled bubble growth contains only the Jakob number and liquid thermal diffusivity value.) However, bubble growth rate has been proven more than once to depend on gravity acceleration [2–5]. There are numerous indications (partially reviewed in ref. [6]) that bubble growth rate is dependent on the liquid Prandtl number and on solid heater material properties. Some works show that the parabolic law for bubble diameter is frequently invalid, and that the diameter is actually proportional to the variable for time raised to a power that may be larger as well as smaller than one half [2, 3, 7]. The dependence of bubble size on Prandtl number can in principle be explained by allowing for liquid flow around the growing bubble [8]. Similarly, the dependence on heater material properties can be understood when direct heat transfer to the bubble through a liquid microlayer beneath the bubble is accounted for [9–12]. There are also possible attempts to explain bubble growth rate dependence on the liquid–vapour surface tension coefficient based on an analysis of microconvective flows that are caused by the thermal and concentrational Marangoni effects [13, 14]. However, growth rate dependence on gravity remains completely incomprehensible.

Bubble detachment size is commonly determined by equating the sum of buoyancy (facilitating bubble detachment) and the effective surface tension force (that is most mistakenly presumed to hinder bubble detachment) to zero. The resultant well-known Fritz formula and its various modifications are deficient for at least two significant reasons. First, they result from applying a static force balance to the essentially unsteady phenomenon of bubble growth and detachment. Second, they give rise to an impossible corollary: that there exists an extended area along which bubble vapour directly borders on the hot surface even at the moment of detachment.

Basing bubble volume calculations at detachment on force balance considerations is also flawed because such considerations do not account for the bubble volume dependence on the heat transfer characteristics that is so frequently observed in experiments. In particular, bubble departure volume was found in refs. [15, 16] to be strongly dependent on a modified Jakob number (with ΔT replaced by T_s), a number

known to have nothing in common with the force balance.

A further hindrance to modelling bubble detachment by means of force balance considerations is the mere fact that the surface tension force does not hold the bubble to the surface but actually adds to buoyancy, thus promoting bubble detachment, as will be proven later in this paper. Interestingly, having met with some discrepancies intrinsic in the notion of that the surface tension force presses the bubble to the surface, Cochran and Aydelott [17] were bold enough to intuitively conclude that there is a net upward "pressure force" that is proportional to the surface tension coefficient and that this force adds to buoyancy, thus facilitating bubble detachment. Although their fundamental premise with regard to surface tension effects seems to be somewhat naive, it happens to be basically true that surface tension force combines with buoyancy to facilitate bubble detachment.

The purpose of this paper is to propose a model that does not contain arbitrary assumptions with respect to the postulated forms of the different forces relevant to vapour bubble evolution. This model will for the first time yield a set of interconnected dynamic equations that describe bubble growth and detachment in a thoroughly rigorous way, providing a springboard that will enable cogent consideration of more complicated vapour bubble dynamics and boiling heat transfer problems in future research efforts.

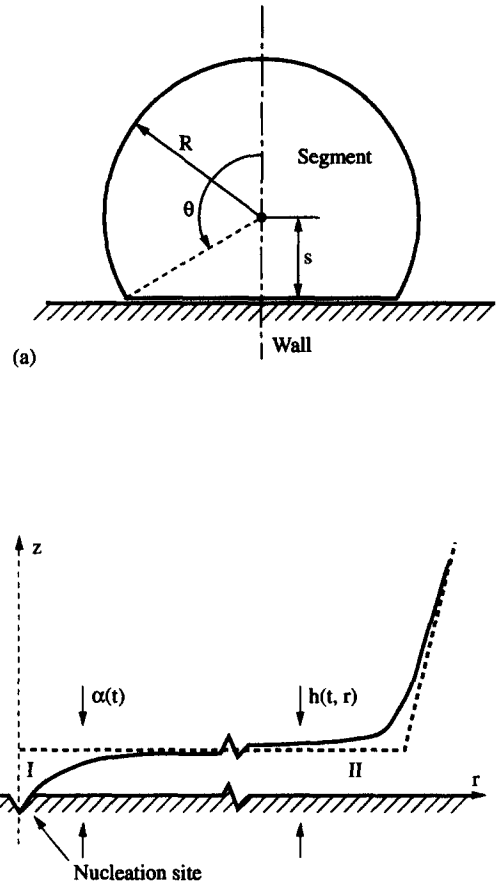

Fig. 1. Schematic of vapour bubble (a) and of microlayer (b).

2. THE PHYSICAL MODEL

In order to avoid unwieldy and tedious calculation and to leave the main ideas unencumbered by unnecessary details, we shall assume from the start that a bubble forming at a nucleation site on an upward facing horizontal wall can be approximately modeled as a spherical segment with a base parallel to the wall, as shown in Fig. 1(a). The segment is separated from the wall by a liquid microlayer whose thickness $h(t, r)$ is very small as compared with radius $R(t)$ of the upper spherical part of the segment [Fig. 1(b)]. This means that the bubble base may be regarded as almost flat irrespective of possible space variations in $h(t, r)$. Only two parameters are needed to define the shape and volume of the segment: radius $R(t)$ and, say, height $s(t)$ of the centre of the curvature of the spherical surface, or perhaps height $z(t)$ of the centre of mass of the segment above the wall, or angle $\theta(t)$ shown in Fig. 1(a). Volume V and total surface area S of the segment, and also z and θ are expressible as

$$V=\frac{4\pi}{3}\left[R^3-\frac{(R-s)^2(2R+s)}{4}\right] \quad S=\pi(R+s)(3R-s)$$

$$z=s+\frac{\pi(R^2-s^2)^2}{4V} \quad \sin\theta=\frac{s}{R}. \tag{1}$$

Arbitrary variations of all variables determining bubble geometry will be significant to the discussion below. We shall express these variations in terms of δV and δz, and these delta values will be regarded as mutually independent. A simple calculation results in

$$\{\delta R, \delta s, \delta\theta\}=\{A_{\mathrm{RV}}, A_{\mathrm{sV}}, A_{\theta\mathrm{V}}\}\,\delta V+\{A_{\mathrm{Rz}}, A_{\mathrm{sz}}, A_{\theta\mathrm{z}}\}\,\delta z$$

$$A_{\mathrm{Rz}}=-\frac{R-s}{2R}A_{\mathrm{sz}}$$

$$A_{\mathrm{RV}}=\frac{1}{2\pi R(R+s)}-\frac{R-s}{2R}A_{\mathrm{sV}}$$

$$\{A_{\theta\mathrm{z}}, A_{\theta\mathrm{V}}\}=\frac{\{A_{\mathrm{sz}}, A_{\mathrm{sV}}\}}{\sqrt{(R^2-s^2)}}-\frac{s\{A_{\mathrm{Rz}}, A_{\mathrm{RV}}\}}{R\sqrt{(R^2-s^2)}}$$

$$A_{\mathrm{sV}}=-\frac{R^2-s^2}{2V}\left(\frac{1}{R+s}-\frac{R^2-s^2}{2V}\right)A_{\mathrm{sz}}$$

$$A_{\mathrm{sz}}=\left[1-\frac{\pi(R+s)^2(R-s)}{2V}\right]^{-1}. \tag{2}$$

The meaning of this assumption is very simple. We substitute real bubble that possesses an infinite degree of freedom number (say, an infinite number of coefficients when representing bubble shape with the help of a series in spherical harmonics) and that must be described by an infinite number of equations by a

segment that possesses only two degrees of freedom, and accordingly, that requires only two equations be used to solve for $V(t)$ and $z(t)$. The same trick was successfully used when describing a liquid droplet approaching a hot wall as a disk in ref. [18].

The microlayer is initially formed when liquid near the wall is left behind as the bubble spreads over the wall and expels liquid ahead of itself. Since the microlayer is very thin, the characteristic time h^2/ν of vorticity diffusion and the characteristic time h^2/χ of temperature diffusion across the microlayer are supposedly much smaller than the time scale of microlayer expansion or reduction along the wall or the timescale of bubble growth. For this reason, liquid flow and heat transfer inside the microlayer may be treated by a quasi-stationary approximation everywhere except at outer region II [the region that immediately adjoins the bubble rim as the bubble advances or retreats in the radial direction, see Fig. 1(b)]. In other words, the fact that the microlayer radial dimension varies as the bubble grows has no appreciable effect on the establishment of velocity and temperature profiles within the main body of the microlayer out of the said marginal region.

For simplicity, evaporation kinetics are assumed sufficiently fast so as to justify our neglecting a possible dependence of phase transition temperature on evaporation rate. Dependence of the phase transition temperature on the curvature of the liquid–vapour interface is ignored as well. (Trivial estimates prove these assumptions to almost always hold approximately true save for some rather esoteric situations.) Given these conditions, temperature may obviously be regarded as uniform along the whole of the interface where vaporization takes place. We further assume that the liquid is devoid of surfactants and other solutes which might affect the surface tension coefficient. This allows us to overlook surface tension gradients resulting from varying solute concentrations near the interface. Thus, the Marangoni effect is entirely excluded from our analysis.

Finally, temperature dependence for both liquid and vapour physical properties is ignored, and wall temperature is taken to be invariable. The latter assumption is approximately valid if the thermal diffusivity of the wall material considerably exceeds that of the adjacent liquid, and if wall material thermal diffusivity is high enough to rapidly compensate both heat absorption due to evaporation and heat removal due to natural convection.

With this range of assumptions in mind, we now focus our attention on the evolution of a single vapour bubble that grows at an isolated nucleation site. And here we make some further assumptions. It is presumed that there is no forced convection. The collective effects usually exhibited in a system of many bubbles are ignored. This means that all effects owing to hydrodynamic and thermal interaction of bubbles near the wall are not at all considered. Likewise, we intentionally confine ourselves to treating the dynamic properties featured by the bubble as it grows and ultimately detaches, without paying attention to the possible influence of those properties on boiling heat transfer characteristics. Investigation of the relation between bubble dynamics and nucleate pool boiling heat transfer requires research methods that are distinctly different from the ones used in the present work. It could constitute a topic of some future paper.

The way in which a bubble evolves can be imagined as follows. Due to liquid vaporization from the bubble spherical surface, as well as from the microlayer, the bubble monotonously grows. Vaporization leads to an increase in $R(t)$, and if angle θ shown in Fig. 1(b) is constant, vaporization also results in a proportional increase in both $s(t)$ and $z(t)$. In cases where θ is constant, the bubble grows without changing its shape. The increase of $R(t)$ and $z(t)$ induces, however, an opposing force due to the inertia of the accelerated liquid. When buoyancy and other forces, if any, that favour the bubble rising above the wall are not large, the inertial force causes the bubble to flatten. This provides an additional reason for broadening of the bubble base, and on the whole, $s(t)/R(t)$ has to decrease in this event. Consequently, the shape of a small bubble, even if the bubble was at first approximately spherical, must progressively deviate from that of a sphere in an early stage of the bubble's growth. But for larger bubble, the forces at play are strong enough to make $s(t)/R(t)$ increase, so that bubble shape becomes more and more spherical as it grows.

The bubble base should normally advance along the wall in the beginning of bubble formation, for one or both of the above indicated reasons. After reaching a maximal area, it must recede during some final stage of bubble evolution and virtually disappear. The moment when the bubble base disappears (and the bubble transforms into a full sphere) may be associated with bubble detachment. Subsequent findings and conclusions corroborate this picture.

3. VARIATION OF MECHANICAL ENERGY

A methodological drawback of the conventionally employed force balance schemes lies in the fact that these forces are evaluated in a haphazard way: they have heretofore been determined by integrating stresses acting on the bubble surface. Such schemes would doubtless be correct if the bubble were a self-contained isolated entity entirely independent of the surrounding liquid. As the matter stands, however, bubble motion is principally inseparable from that of the surrounding liquid. This is unequivocally confirmed by the mere fact that forces opposing either bubble growth or bubble translational motion are primarily associated with inertia of the liquid being expelled as the bubble expands, or with inertia of the virtual liquid mass being carried along as the bubble moves. This means that an analysis of momentum conservation should be conducted with respect to the whole system under study, a system that would include

both the bubble and the ambient liquid, rather than a system which would take the bubble in isolation.

The forces that govern bubble behaviour may vary as the bubble evolves. Some of these forces affect bubble expansion, whereas other ensure its translational motion. It is often difficult to distinguish between forces that bear upon bubble expansion and those which have relevance to bubble translational motion for the simple reason that bubble development entails substantial changes in bubble shape. For instance, the inertia of the liquid displaced by the growing bubble either resists or assists expansion, depending on the course of bubble development. If the bubble centre of mass is positioned at a fixed point the bubble expansion is spherically symmetric, there are no changes in bubble shape. However, space accessible to the bubble is restricted by the solid wall. Hence the centre of mass should inevitably shift above the wall as the bubble grows, even if bubble shape were maintained invariable. Accordingly, liquid expansion caused by bubble growth loses its spherical symmetry, and the appearance of a corresponding inertial force which is due solely to liquid expansion and which influences a shift of the bubble centre can readily be anticipated. This inertial force contributes to the action of the familiar inertial force which itself is due to the virtual mass of liquid that is carried along by the moving bubble and which resists bubble translational motion.

Surface tension effects at the liquid–vapour interface also vary as the shape of the interface varies. These effects not only oppose bubble growth through the action of an extra pressure drop across the curved bubble surface, but they must also favour any change in bubble shape that leads to a decrease of the total bubble surface area at a given bubble volume. Inasmuch as any such change in bubble shape is accompanied by a displacement of the bubble centre of mass, as is the case for vapour bubbles in nucleate pool boiling, surface tension necessarily brings about an additional force that helps to promote this displacement.

At present, we have no clear means of distinguishing translational forces from expansional ones. To resolve this problem, we apparently have to resort to the general thermodynamic method, in accordance with which we must consider a variation of a suitable thermodynamic potential, and this variation must be presented as the sum of generalized thermodynamic forces multiplied by variations of corresponding generalized thermodynamic variables. If this potential is invariable during the bubble evolution process, and if the thermodynamic variable variations are independent, then all generalized thermodynamic forces must turn to zero. In this way, a set of equations that govern bubble development can be obtained, the total number of these equations being equal to the number of thermodynamic forces.

As has already been pointed out, the system under study possesses two degrees of freedom, so we need but introduce two independent variables. It is best to choose V and z to represent those variables, and to suppose that the total mechanical energy of the whole system is a relevant thermodynamic potential which remains invariable at an arbitrary virtual variation of these variables. In order to regard the system's total mechanical energy as an invariable quantity, we need (1) to neglect viscous dissipation of kinetic energy and (2) to formally set the variation of total vapour mass within the bubble to zero during evaluation of mechanical energy variation. Viscous dissipation may be safely ignored for reasons indicated later. Vapour mass variation must be formally set to zero since evaporation evokes a partial transformation of thermal energy into mechanical energy, and the mechanical energy of the whole liquid-bubble system would not vary during bubble evolution only under the condition of this transformation being entirely discarded.

The mechanical energy of the system consists of two kinetic energy and three potential energy components. The kinetic energy components are due to: (1) displacement of the bubble centre of mass in translational motion; this gives way to bubble vapour acceleration and acceleration of the additional liquid mass and (2) bubble expansion; this results in a roughly radial motion of liquid and vapour. The potential energy components involve: (1) system potential energy in the gravity field, (2) surface tension energy and (3) vapour compression energy within the bubble.

3.1. *Kinetic energy*

Kinetic energy variation associated with bubble translational motion can be formulated in a straightforward manner, by its very definition,

$$\delta E_1 = \frac{\mathrm{d}}{\mathrm{d}t}\left[\left(\rho_v + \frac{k(\theta)}{2}\rho_l\right)V\frac{\mathrm{d}z}{\mathrm{d}t}\right]\delta z \tag{3}$$

where $k(\theta)$ is a virtual mass coefficient. This coefficient equals unity for a sphere moving in an unbounded fluid and 11/8 for a sphere touching a solid plate as it begins to move normally to the plate [19].

If bubble expansion is taken to be spherically symmetric, liquid radial velocity equals $w_l = (R/r)^2(\mathrm{d}R/\mathrm{d}t)$, and kinetic energy variation of the liquid associated with bubble expansion would be

$$\delta E_{2l} \equiv \delta\left\{\tfrac{1}{2}\rho_l\int_{r>R}\left[\left(\frac{R}{r}\right)^2\frac{\mathrm{d}R}{\mathrm{d}t}\right]^2\mathrm{d}V\right\}$$

$$= 4\pi\rho_l R^2\left[R\frac{\mathrm{d}^2R}{\mathrm{d}t^2} + \frac{3}{2}\left(\frac{\mathrm{d}R}{\mathrm{d}t}\right)^2\right]\delta R.$$

If the bubble is a spherical segment, E_{2l} can be approximated as

$$E_{2l} = (1-\cos\theta)K_l(\theta)\rho_l R^3(\mathrm{d}R/\mathrm{d}t)^2$$

with $K_l(\theta)$ being understood as a correction function that accounts for the presence of the boundary wall parallel to the segment base. If the bubble is a growing

sphere touching the wall, then $\theta = \pi$, $1-\cos\theta = 2$, and $K_l(\pi) = 14/3$ [20], which values have been utilized previously by Mikic *et al.* [1]. For a sphere far away from the wall $K(\pi) = \pi$, and we obtain the former result for spherically symmetric expansion (which is represented within the curly brackets in the preceding equation for δE_{2l}). When the bubble is a radially growing hemisphere attached to the wall, and if the viscous boundary layer is neglected, then $\theta = \pi/2$, $1-\cos\theta = 1$, and again $K_l(\pi/2) = \pi$. After manipulation, variation of E_{2l} can be formally designated as

$$\delta E_{2l} = 2(1-\cos\theta)K_l(\theta)\rho_l R^2\left[R\frac{d^2R}{dt^2}+\frac{3}{2}\left(\frac{dR}{dt}\right)^2\right]\delta R + \frac{d}{d\theta}[(1-\cos\theta)K_l(\theta)]\rho_l R^3\left(\frac{dR}{dt}\right)^3\delta\theta. \quad (4)$$

While calculating the corresponding kinetic energy of bubble vapour, we assume vapour density to be uniform throughout the bubble. This forces the continuity equation to yield, for a spherically symmetric flow, the following expression for the vapour radial velocity: $w_v = (r/R)(dR/dt)$. The total mass of vapour inside the bubble has been formally taken constant while dealing with the continuity equation in conformity with the requirement indicated above, that is, $\delta(\rho_v V) = 0$. Allowing for the restricting wall in the same manner as before, we now get

$$E_{2v} = (1/5)(1-\cos\theta)K_v(\theta)\rho_v R^3(dR/dt)^2$$

and, instead of equation (4),

$$\delta E_{2v} = \frac{2}{5}(1-\cos\theta)K_v(\theta)\rho_v R^2\left[R\frac{d^2R}{dt^2}+\frac{3}{2}\left(\frac{dR}{dt}\right)^2\right]\delta R + \frac{1}{5}\frac{d}{d\theta}[(1-\cos\theta)K_v(\theta)]\rho_v R^3\left(\frac{dR}{dt}\right)^3\delta\theta. \quad (5)$$

The desired variation δE_2 of kinetic energy attributable to bubble expansion is obtained by summing equations (4) and (5).

3.2. *Potential energy*

If the potential energy of a liquid without any bubbles is taken as zero, then the potential energy of liquid and vapour in the gravity field can be represented as $U_g = -(\rho_l-\rho_v)Vgz+\text{const}$. Hence, again taking as invariable the total vapour mass,

$$\delta U_g = -(\rho_l-\rho_v)Vg\,\delta z-\rho_l gz\,\delta V. \quad (6)$$

By definition, the potential energy of surface tension equals $U_\sigma = \sigma S$, whence

$$\delta U_\sigma = \sigma\,\delta S = 2\pi\sigma[(3R+s)\,\delta R+(R-s)\,\delta s]. \quad (7)$$

The potential energy assigned to vapour compression can be most conveniently expressed in terms of the virtual work performed by the vapour as the bubble grows. This yields

$$\delta U_c = -\oint_S (p_v-p_\infty)\,\delta n\,dS$$

where integration is performed over the whole bubble surface, p_∞ is liquid pressure at infinity, and δn is the virtual local displacement of the surface. Evidently, $\delta n = \delta R+(\cos\theta)\,\delta s$ at the spherical portion of the bubble boundary, and $\delta n = 0$ at the bubble base. Thus,

$$\delta U_c = -\pi R^2(p_v-p_\infty)[2(1-\cos\theta)\,\delta R+\sin^2\theta\,\delta s]. \quad (8)$$

As a final result, the mechanical energy conservation law yields

$$\delta E_1+\delta E_2+\delta U_g+\delta U_\sigma+\delta U_c = 0. \quad (9)$$

All the terms involved in this fundamental variational equation are specified in equations (3)–(8). They contain variations δR, δs and $\delta\theta$ which have to be expressed through variations δV and δz with the aid of equation (2). Since the latter variations can be duly regarded as mutually independent, equation (9) in fact splits into two dynamic equations governing bubble growth and motion of its centre of mass.

4. DYNAMIC EQUATIONS

After simple manipulation, dynamic equations describing bubble expansion and translational motion can be formulated as follows:

$$2(1-\cos\theta)(K_l(\theta)\rho_l+\tfrac{1}{5}K_v(\theta)\rho_v)R^2\left[R\frac{d^2R}{dt^2}+\frac{3}{2}\left(\frac{dR}{dt}\right)^2\right]A_{RV}+\frac{d}{d\theta}[(1-\cos\theta)(K_l(\theta)\rho_l+\tfrac{1}{5}K_v(\theta)\rho_v)]R^3\left(\frac{dR}{dt}\right)^2A_{\theta V} = p_v-(p_\infty-\rho_l gz)-\frac{\sigma}{R}\left[\frac{3R+s}{R+s}-\pi(R^2-s^2)A_{sV}\right] \quad (10)$$

$$\frac{d}{dt}\left[\left(\rho_v+\frac{k(\theta)}{2}\rho_l\right)V\frac{dz}{dt}\right]+2(1-\cos\theta)\times(K_l(\theta)\rho_l+\tfrac{1}{5}K_v(\theta)\rho_v)R^2\left[R\frac{d^2R}{dt^2}+\frac{3}{2}\left(\frac{dR}{dt}\right)^2\right]A_{Rz}+\frac{d}{d\theta}[(1-\cos\theta)(K_l(\theta)\rho_l+\tfrac{1}{5}K_v(\theta)\rho_v)]R^3\left(\frac{dR}{dt}\right)^2A_{\theta z} = (\rho_l-\rho_v)Vg+\frac{\pi(R^2-s^2)\sigma}{R}A_{sz}. \quad (11)$$

The quantities s, z, θ, R and V have been defined in Section 2 of this paper. They are related to each other by three equations (1). This means that any two of

these five quantities may be regarded as independent and taken as unknown variables of the above equations.

Equation (10) is the dynamic equation describing bubble expansion. Its left-hand side corresponds to an effective inertial force that is essentially dependent not only on bubble size but also on current bubble shape. The first term on the right-hand side represents an effective pressure drop that drives bubble expansion. Allowance for contribution $\rho_l g z$ to this term makes more precise the value of liquid pressure that should be used when formulating this pressure drop. The physical meaning of the gravity correction to p_∞ is quite obvious and requires no further explanation. The second term on the right-hand side of equation (10) stems from surface tension at the bubble boundary surface. It is also dependent on bubble shape. Note that this term considerably deviates from the familiar quantity $2\sigma/R$ which is characteristic of spherical interfaces and which is universally introduced when attempting to make a correction to the pressure drop due to surface tension. However, this second term tends to $2\sigma/R$ as s approaches R, that is, as the bubble transforms into an undeformed sphere.

Equation (11) describes translational motion of the deformed bubble. The left-hand side of this equation involves two inertial terms of different physical origin. The first term comes from vapour acceleration inside the bubble and acceleration of the virtual mass of liquid. The second term describes inertia of the liquid being placed into motion as the bubble grows, and inertia of expanding vapour flow. The corresponding inertial force is the result of the fact that the spherical symmetry of liquid and vapour flow is broken because the bubble borders on the solid wall. The last force may be conceived, in a sense, as a specific reaction force exerted by the wall.

Only two forces affecting bubble motion appear on the right-hand side of equation (11). The first term is rather trivial: it represents the buoyancy that is used in calculations dealing with vapour and gaseous bubbles. The second term is entirely novel. It represents an effective surface tension force that until now has not been taken into account in a concise manner. This surface tension force helps the bubble to attain spherical form and so favours the rise of its centre over the wall. This means that it adds to the action of buoyancy in facilitating bubble detachment. The physical origin of the surface tension force is analogous to that of the familiar elastic force that occurs when an elastic sphere, such as a rubber ball, is pressed against a solid plate. Just as the latter force causes the elastic sphere to rebound from the plate, the former surface tension force causes the bubble to detach. Our derivation of such a surface tension force that facilitates bubble detachment is contrary to the unfounded presumptions and inferences in numerous papers in the field which generally suppose surface tension effects to originate a net force that keeps the bubble attached to the wall and, thus, impedes detachment.

An approach similar to that presented above has proven successful in resolving a difficult problem that involves the dynamic and thermal interaction of a deformable liquid droplet impinging onto a superheated surface [18]. In this case, analysis of potential energy variations exhibited due to surface tension has led to the unequivocal conclusion that a surface tension force exists, and that this force helps the droplet to restore its original spherical shape. This force has been shown to play a very significant role when explaining the dynamic Leidenfrost phenomenon which is so important in the design of manifold spray cooling processes.

It should be emphasized that our fundamental inference about surface tension force facilitating bubble detachment is entirely independent of all the assumptions made to simplify our analysis. All these assumptions can be avoided at the cost of making calculations more complicated and tedious, and none of them affects in the least the above derivation of dynamic equations from the mechanical energy conservation law. In this respect, the inference that the surface tension force facilitates bubble detachment is rigorous, and it is crucial for studies of vapour bubble dynamics. Moreover, this inference evidently invalidates principal conclusions pertaining to bubble detachment in other known theoretical papers on this subject which invariably treat the surface tension force as a force pressing the bubble to the wall. Hence follows another obvious inference that those priorly drawn conclusions must be revised.

As might well be expected in light of the Curie principle of the thermodynamics of irreversible processes, the pressure drop between vapour within the bubble and the ambient liquid does not originate a force that would bear upon bubble translational motion. It is not surprising, therefore, that the corresponding contribution to compression energy variation in equation (8) that is proportional to δz can readily be shown to be identically equal to zero.

For good reasons, equation (11) does not include a term to describe any force that might arise from the momentum of vapour molecules emerging from the bubble boundary as a result of evaporation. The vapour momentum imparted to the bubble ultimately comes from the evaporating liquid, and the momentum conservation equation unambiguously requires it to be exactly compensated by a corresponding liquid momentum loss. This means that there should be no momentum change in the whole system, and consequently, no ensuing force that would be capable of affecting system behaviour. This state of affairs is in contrast to those discussed in some papers (for example, see ref. [4]). This situation is drastically different from that encountered in processes where bubbles are formed as a result of gas being injected into a liquid through submerged nozzles or plate orifices. In the latter case, some amount of momentum is brought into the system from outside, that is, with flow of the injected gas, and this momentum inflow results in the

occurrence of a force that is precisely equal to the total momentum flux, again in compliance with the momentum conservation law.

In our application of the energy conservation law, we have purposefully omitted consideration of a drag force, and its corresponding viscous dissipation of kinetic energy. A drag coefficient could be assigned to a bubble if a wake were completely established behind the bubble. As the matter stands, there is no "behind" for a bubble attached to a wall, and even if there were, initial bubble motion would be practically irrotational anyway [21]. Consequently, the wake would not be fully developed until the bubble had covered an appreciable distance, one comparable to its linear size. It is not surprising therefore that drag force has been generally found to be negligible with respect to the evolution of either gaseous bubbles formed in the process of gas injection [19], or vapour bubbles in nucleate pool boiling [3]. At the same time, viscous stresses displayed near a moving liquid–gas or liquid–vapour interface may usually be ignored, saving in rather special situations.

It should be pointed out that equations (10) and (11) are somewhat devaluated by the fact that too little is known about functions $k(\theta)$, $K_l(\theta)$ and $K_v(\theta)$ which appear in these equations. However, these equations can be approximately formulated for bubbles whose shape is close either to a hemisphere ($\theta \approx \pi/2$) or to a sphere ($\theta \approx \pi$).

5. MICROLAYER

Equation (11) includes one extra unknown variable: vapour pressure p_v. Using the linearized Clapeyron–Clausius equation, we can reduce this variable to bubble vapour temperature T_v, which is unknown as well. Thus a complementary equation that expresses heat transfer to the growing bubble is necessary to render the set of equations (10) and (11) completely closed, as has been explained in detail in ref. [1]. Solution of the heat transfer problem usually leads to a relation between dR/dt and temperature differences $T_w - T_s$ and $T_\infty - T_s$ which closes the set of dynamic equations.

When formulating a heat transfer equation, we must account for the fact that heat is transferred to the liquid–vapour interface not only from the bulk of superheated liquid, but also directly from the wall, through the liquid microlayer underneath the bubble [9, 10, 22]. For this reason, we need to consider flow and heat transfer within the microlayer.

The Peclet number characterizing convective heat transport in the microlayer can be proven to be very small compared with unity. This means that convective transport can be neglected and only heat conduction has to be taken into account. Since temperature variations in the direction normal to the wall greatly exceed those in the longitudinal direction due to the microlayer being extremely thin, the quasi-stationary temperature profile in the microlayer is expressible as

$$T(z:t,r) \approx T_w - [z/h(t,r)]\,\Delta T \quad \Delta T = T_w - T_s \tag{12}$$

where $h(t,r)$ is microlayer thickness.

Equation (12) completely determines the heat flux from the wall to the microlayer free surface, and consequently, the amount of liquid per unit area that is evaporated there in a unit time. As a result, liquid and vapour normal velocities at the surface are to be written out as follows:

$$w_l = \frac{\gamma}{h} \quad w_v = \frac{\gamma}{\kappa h} \quad \gamma = \frac{\lambda \Delta T}{\rho_l L} \quad \kappa = \frac{\rho_v}{\rho_l}. \tag{13}$$

Thus, the problem of calculating vapour flux to the bubble through its lower boundary is reduced to the problem of determining microlayer thickness.

With the exception of marginal regions which adjoin (1) the nucleation site where the bubble first originates and (2) the advancing or retreating bubble meniscus [regions I and II of Fig. 1(b)], the microlayer is thin in the sense that liquid velocity varies in the lateral direction much faster than in the longitudinal radial direction. This means that governing fluid dynamic equations may be formulated as a familiar boundary layer approximation, the same approximation which is generally used in studies of thin fluid films. Thus,

$$\frac{\partial w_r}{\partial t} + w_r \frac{\partial w_r}{\partial r} + w_z \frac{\partial w_r}{\partial z} = \nu \frac{\partial^2 w_r}{\partial z^2} - \frac{1}{\rho_l} \frac{\partial p}{\partial r}$$

$$\frac{\partial p}{\partial z} = 0 \quad \frac{\partial (r w_r)}{\partial r} + \frac{\partial (r w_z)}{\partial z} = 0. \tag{14}$$

These equations assume that the liquid is incompressible. Pressure variations due to gravity which are irrelevant in a thin layer are also overlooked.

Our actual realm of interest bears upon averaged microlayer characteristics: microlayer thickness and the mean radial velocity of the liquid within the microlayer. It suggests that equation (14) be integrated over dz across the whole microlayer. By so doing, we are following a universal procedure recently applied to axisymmetric liquid films spreading over a flat surface [23]. Boundary conditions assumed while looking for solutions to equation (14) are of a standard form,

$$w_r = w_z = 0 \quad z = 0, \quad w_z = \frac{\partial h}{\partial t} + w_r \frac{\partial h}{\partial r} + \frac{\gamma}{h}$$

$$\frac{\partial w_r}{\partial z} = 0 \quad p = \text{const}, \quad z = h(t,r) \tag{15}$$

where p is a uniform pressure along the microlayer free surface. This value is slightly different from the vapour pressure inside the bubble which is due to the momentum carried away by vapour molecules that are emitted by the surface, and to a small radial variation of the surface curvature. The microlayer is sup-

posed not too thin for disjoining pressure to play a noticeable role.

The conditions imposed at the boundary between the microlayer and the wall are the usual no-slip boundary conditions. The first of the above conditions at the free microlayer surface is the familiar kinematic condition with an allowance made for the vaporization of inflowing liquid. The second of the above conditions suggests the interface to be force-free. Among other things, the last condition implies that there are no significant temperature and surfactant concentration gradients along the interface. The third condition at $z = h(t,r)$ corresponds to a neglect of surface tension effects at the almost flat interface as well as of inertial effects in the vapour that fills the bubble.

The integration of equation (14) with allowance for requirements (15) yields

$$\frac{\partial}{\partial t}\int_0^h w_r\,dz+\frac{1}{r}\frac{\partial}{\partial r}\left(r\int_0^h w_r^2\,dz\right)+\frac{\gamma}{h}\int_0^h w_r\,dz = -\nu\left.\frac{\partial w_r}{\partial z}\right|_{z=0},$$

$$\frac{\partial h}{\partial t}+\frac{1}{r}\frac{\partial}{\partial r}\left(r\int_0^h w_r\,dz\right)+\frac{\gamma}{h}=0. \qquad (16)$$

Thus, unknown variable w_z is excluded at the expense of introducing another unknown variable: microlayer thickness h.

It is natural to next make use of the well-known Karman–Polhausen method according to which the radial velocity component is expressed in the self-similar form,

$$w_r=\frac{3}{2}\left(\eta-\frac{1}{3}\eta^3\right)u \quad \eta=\frac{z}{h} \qquad (17)$$

compatible with the remaining equations (15). Thus, variable w_r is also replaced by a new variable, the mean radial velocity u.

After performing the integration in equation (16) with the help of profile (17), we arrive at a set of nonlinear equations,

$$\frac{5}{8}\frac{\partial}{\partial t}(hu)+\frac{17}{35}\frac{1}{r}\frac{\partial}{\partial r}(rhu^2)+\left(\frac{3}{2}\nu+\gamma\right)\frac{u}{h}=0$$

$$\frac{\partial h}{\partial t}+\frac{5}{8}\frac{1}{r}\frac{\partial}{\partial r}(rhu)+\frac{\gamma}{h}=0. \qquad (18)$$

A comprehensive analysis of equations (18) would prove difficult to perform for two main reasons: (1) the strongly nonlinear nature of the equations and (2) uncertainties encountered when formulating a boundary condition at $r = 0$ because this boundary condition is dictated by unknown peculiarities of a particular nucleation site. We shall avoid these difficulties by looking for a partial solution to equations (18) belonging to the following type:

$$h(t,r)=\alpha(t)r^n \quad u(t,r)=\beta(t)r^m. \qquad (19)$$

By substituting these relations into equation (18) we get $n = 0$, $m = 1$, and further,

$$\beta=-\frac{4}{5\alpha}\left(\frac{d\alpha}{dt}+\frac{\gamma}{\alpha}\right),$$

$$\frac{d}{dt}\left(\frac{d\alpha}{dt}+\frac{\gamma}{\alpha}\right)-\frac{1632}{875\alpha}\left(\frac{d\alpha}{dt}+\frac{\gamma}{\alpha}\right)^2+\frac{8}{5\alpha^2}\left(\frac{3}{2}\nu+\gamma\right)\left(\frac{d\alpha}{dt}+\frac{\gamma}{\alpha}\right)=0.$$

When solving the above ordinary differential equation for α, we dismiss as physically incongruous both irrelevant constant solutions and solutions that tend to a constant as t goes to infinity. Moreover, we require that a relevant solution be zero at $t = 0$ and that it remain finite at any instant, that is, we require $\alpha < \infty$ at $t \to \infty$. Then we obtain, as a final result,

$$h=H\sqrt{(\nu_e t)} \quad u=-\frac{2}{5}\frac{r}{t} \quad H=\left(\frac{4200}{2507}\right)^{1/2}\approx 1.294,$$

$$\nu_e=\nu-\frac{58}{525}\gamma\approx\nu-0.11\gamma. \qquad (20)$$

It is quite suggestive that only solution (20) that describes a microlayer of uniform thickness is derivable from among all other possible profiles prescribed by equations (19). This confirms to an extent the expectation that the microlayer is flat everywhere except at the marginal region adjoining the nucleation site and at the moving fringe of the bubble meniscus. This solution is especially striking because mean velocity $u(t,r)$ is totally independent of liquid viscosity, despite the fact that flow inside the microlayer is essentially viscous. This indicates that the liquid being left behind as the bubble meniscus advances along the wall makes for a kinematic origin of the flow. However, the more viscous the liquid and the weaker the evaporation, the larger the microlayer thickness. As unexpected as it may seem, microlayer thickening is implicitly confirmed by the very fact that bubble volume increases roughly proportional to the square root of time, at least in cases where vaporization at the free microlayer surface prevails in providing for bubble growth as compared with evaporation from the bulk.

The rate with which microlayer thickness increases is proportional to an effective kinematic viscosity ν_e that decreases with γ, so that there is a critical value of the evaporation rate corresponding to $\gamma_{cr} \approx 9.05\,\nu$. If an actual γ exceeds this threshold value, there is altogether no solution to equations (18) of the type specified in equation (19). This means that evaporation will be strong enough to prevent the formation of a microlayer beneath the bubble from the very beginning of bubble development. This critical threshold value of γ may justifiably be associated with the well-known burnout crisis, although a dry spot

near the nucleation site can make its appearance spontaneously at evaporation rates corresponding to considerably smaller γ.

One might think that equations (20) contradict experiments in which it was inferred that the liquid microlayer beneath the vapour bubble is almost wedge-shaped, with its thickness decreasing as the bubble grows [9–12]. Moreover, in these experiments, a dry spot around the nucleation site was detected that broadened with time, due to evaporation. But when we consider that equations (20) should be viewed as bearing upon averaged microlayer thickness and upon velocity outside of the marginal regions mentioned above, there is no real contradiction.

Notwithstanding, we must be cautious when applying the above results to a final stage of bubble evolution, that is, the stage in which the bubble base is likely to reduce. Admittedly, equations (20) should hold true for an early stage during which the advancing bubble meniscus leaves behind some amount of liquid in the vicinity of the wall. However, it is doubtful whether these equations may be acceptable for the final stage when the meniscus retracts, because there is no apparent physical reason for liquid to flow into the microlayer from the outside. It seems much more probable that the liquid inflow ought to terminate at such a stage, so that the regime of microlayer thickening specific to the initial and intermediate periods of bubble growth is replaced by a regime of microlayer thinning.

In addition, we have imposed no boundary conditions at the nucleation site. Admittedly, microlayer thickness at the nucleation site must turn to zero at the initial moment of bubble origination, and this fact has been entirely ignored when looking for solutions in the form of (19). Therefore, bubble thickness near the nucleation site must (1) be very small, so that molecular attraction forces that give rise to disjoining pressure become important and (2) vary with the radial coordinate sufficiently fast to render the surface tension contribution to pressure within the microlayer significant as well. Both these reasons can easily be proven to make for the appearance and subsequent broadening of a dry spot around the nucleation site.

The net gain of this section consists in the conclusion that heat flux across the microlayer to a unit area of the lower bubble boundary equals

$$q_m = \lambda \Delta T / h(t) \tag{21}$$

with $h(t)$ identified by equation (20).

6. THERMALLY CONTROLLED BUBBLES

In the remainder of this paper, we apply the above-developed dynamic theory for vapour bubble growth and detachment to the simplest possible case where bubble growth is thermally controlled, and consequently, all inertial effects, however significant for motion of the bubble centre of mass, are entirely irrelevant with respect to bubble expansion. For thermally controlled bubbles, the averaged heat flux density to the upper spherical part of the bubble surface from the bulk of the ambient superheated liquid can be formulated in a form similar to that of equation (21),

$$q_b \approx \lambda \Delta T / l(t) \quad l(t) = (2/C)\sqrt{(\chi t)} \tag{22}$$

where constant C appears in the classical parabolic law for bubble growth, which is formulated as

$$R(t) = CJa\sqrt{(\chi t)}. \tag{23}$$

A great many papers and textbooks contain review of the various values for C that can be obtained within the framework of differing models of bubble growth within a superheated liquid layer near the wall. Most of these values fall within the range of 1–2. However, formula (23) may also be regarded as an empirical correlation which holds approximately true even for boiling of subcooled liquids. In this case, C must be regarded as an empirical constant which may have a value smaller than unity.

When bubble growth is thermally controlled, dynamic equation (10) for bubble expansion is utterly irrelevant. The bubble growth equation can be formulated immediately as follows:

$$\frac{dV}{dt} = \left[\frac{2\pi R(R+s)}{l(t)} + \frac{\pi(R^2 - s^2)}{h(t)}\right]\frac{\lambda \Delta T}{\rho_v L}.$$

This equation relates the bubble growth rate to the rate of heat transfer divided by the vapour density inside the bubble. The first term in brackets is proportional to the heat flux to the spherical part of the bubble surface from the bulk of liquid in accordance with equation (22). The second term represents heat transfer to the lower bubble surface through the microlayer in accordance with equation (21). Taking into account the equations for $l(t)$ and $h(t)$, the bubble growth equation can be reformulated as

$$\frac{dV}{dt} = \pi R(R+s)\left(1 + N_m \frac{R-s}{R}\right) CJa\left(\frac{\chi}{t}\right)^{1/2}$$

$$N_m = \frac{1}{CH}\left(\frac{\chi}{\nu}\right)^{1/2} \equiv \frac{1}{CHPr^{1/2}} \tag{24}$$

where parameter N_m stands for a new dimensionless criterion that specifies the relative importance of vaporization at the microlayer free surface. The larger N_m, the more important the heat transfer contribution by heat conduction through the microlayer, and this is all the more true for almost hemispherical bubbles for which $s \approx 0$.

Equations (11) and (24) constitute a closed set of equations used to solve for both R and z. As has already been indicated, a stumbling block to solving this set is met with the regrettable fact that equation (11) contains coefficients $k(\theta)$, $K_l(\theta)$ and $K_v(\theta)$ which are approximately known only for those bubbles close in shape either to a sphere or to a hemisphere.

When the bubble is almost hemispherical, equations (11) and (24) reduce to

$$\frac{dR}{dt} = \tfrac{1}{2}CJa(1+N_m)\left(\frac{\chi}{t}\right)^{1/2}$$

$$R(t) = CJa(1+N_m)\sqrt{(\chi t)}+\text{const} \qquad (25)$$

and

$$\frac{d}{dt}\left(R^3\frac{dz}{dt}\right)=\left[\frac{k(\pi/2)}{2}+\kappa\right]^{-1}\left\{(1-\kappa)R^3 g\right.$$

$$\left.+6R\sigma+6\left(1+\frac{\kappa}{5}\right)R^2\left[R\frac{d^2R}{dt^2}+\frac{3}{2}\left(\frac{dR}{dt}\right)^2\right]\right\} \qquad (26)$$

with $k(\pi/2)$ being an unknown value describing the virtual mass coefficient for a growing hemisphere attached to a flat surface.

Three forces appear in the right-hand side of equation (26): buoyancy, an effective force due to surface tension, and a force resulting from inertia of the liquid displaced by the expanding hemisphere. The two former forces are positive and accordingly favour the bubble centre rising above the wall, whereas the latter force can be shown to be negative with the aid of equation (25). This means that the force due to liquid inertia makes for flattening the bubble and tries to keep it near the wall.

When the bubble is almost spherical, we arrive at the following equations, instead of equations (25) and (26),

$$\frac{dR}{dt} = \tfrac{1}{2}CJa\left[1+\left(N_m-\frac{1}{2}\right)\frac{R-s}{R}\right]\left(\frac{\chi}{t}\right)^{1/2}$$

$$R(t) \approx CJa\sqrt{(\chi t)} \quad \text{at} \quad N_m \leqslant 1 \qquad (27)$$

and

$$\frac{d}{dt}\left(R^3\frac{ds}{dt}\right)=\frac{16}{11}\frac{1-\kappa}{1+a\kappa}R^3 g$$

$$+\frac{12}{11(1+a\kappa)}\frac{R^2-s^2}{R}\frac{\sigma}{\rho_l} \quad a=\frac{16}{11}. \qquad (28)$$

Variable s may be substituted for z in the last equation which can, of course, also be made linear within the same limits of accuracy by setting $R^2-s^2 \approx 2R(R+s)$. The force due to inertia of the expanding liquid can be proven to be proportional to the small bubble base area, $\pi(R^2-s^2)$. Since this force is necessarily small, it may be overlooked in light of the large inertial force on the left-hand side of equation (28). In this case, only buoyancy and surface tension remain to affect bubble evolution, and both of them assist the bubble in detaching from the wall. The force due to buoyancy is negligible as compared with force due to surface tension for sufficiently small bubbles. However, the former force increases and can eventually become dominant over the latter force as the bubble grows.

We have already pointed out that a vapour bubble evolving at a nucleation site is likely to be close in shape to a hemisphere at some early stage of its development and to a sphere immediately before detachment. This suggests that a two-stage bubble growth model could possibly be put forward by analogy with a similar model for the formation of gaseous bubbles at a submerged plate orifice [24]. The first stage is assumed to correspond to the growth of an almost hemispherical vapour envelope that is pressed to the wall by the inertial force generated at its expanding external boundary. When the force balance is reversed, a second stage takes place in which buoyancy and surface tension forces prevail over the liquid inertial force. After a relatively short time elapses, the bubble may be approximately viewed as an equivalent sphere of the same volume (cf. the gas injection model in refs. [19, 24]).

The duration t_1 of the first stage can be found by equating the right-hand side of equation (26) to zero. This gives an algebraic equation, with allowance for the parabolic law (25),

$$t_1^{3/2}+\frac{6}{(1-\kappa)[CJa(1+N_m)]^2}\frac{\sigma/\rho_l}{g\chi}t_1^{1/2}$$

$$=\frac{3}{4}\frac{(1+\kappa/5)CJa(1+N_m)}{1-\kappa}\frac{\chi^{1/2}}{g}.$$

If buoyancy dominates or if the Jakob number is high, t_1 is scaled with $\chi^{1/3}g^{-2/3}$ and is proportional to $Ja^{2/3}$. For the opposite limiting case in which the surface tension force prevails or the Jakob number is low, t_1 scales with $\chi^3(\sigma/\rho_l)^{-2}$ and is proportional to Ja^6.

No matter whether buoyancy or surface tension dominates, t_1 can be shown to be small as compared with the whole period of bubble evolution up to the moment of detachment. The relative duration of the first development stage for vapour bubbles in nucleate boiling happens to be much smaller than that for gaseous bubbles formed as a result of gas injection through nozzles or orifices. (For gas-injected bubbles, the first stage amounts to up to twenty per cent of the entire bubble evolution process [24].) The difference between the duration of the second stage for gas-injected vs nucleate boiling bubbles is due to the fact that vapour bubble growth rate depends on bubble surface area. Bubble growth rate is relatively negligible for vapour bubbles, provided they are sufficiently small, as compared with the growth rate of those gaseous bubbles into which gas usually flows with an almost invariable discharge.

Since the first stage of bubble development is short, we are afforded an opportunity to altogether ignore the extent to which bubble shape deviates from that of a sphere at the first initial stage, and instead we approximately assume the bubble to be nearly spherical, as is often assumed even when treating gaseous bubble formation [19].

Thus, with a mind to develop a comparatively sim-

ple model of bubble growth and detachment, we must now consider solutions to equations (27) and (28).

7. BUBBLES WITH NEGLIGIBLE EVAPORATION FROM THE MICROLAYER

If parameter N_m involved in equation (27) is not too large compared with unity (meaning in view of its definition in equation (24) that Pr is not too low), evaporation from the base of nearly spherical bubbles may be ignored. In this case, equation (27) yields the known parabolic law of bubble growth, and we have to deal with the only equation (28) that must be solved to find s.

7.1. *Bubbles dominated by buoyancy*

If buoyancy plays a major role in promoting the rise of bubble above the wall, it is natural to introduce time and length scales based on a comparison of the first term on the right-hand side of equation (28) and the inertial force on the left-hand side. Thus we choose to define

$$t = L_t^{(b)}\tau$$

$$L_t^{(b)} = \left(\frac{11}{16}\frac{1+a\kappa}{1-\kappa}\right)^{2/3}\left(\frac{CJa\sqrt{\chi}}{g}\right)^{2/3} \approx 0.779\frac{(CJa)^{2/3}\chi^{1/3}}{g^{2/3}}$$

$$s = L_s^{(b)}\zeta$$

$$L_s^{(b)} = \left(\frac{11}{16}\frac{1+a\kappa}{1-\kappa}\right)^{1/3}\frac{(CJa\sqrt{\chi})^{4/3}}{g^{1/3}} \approx 0.883\frac{(CJa)^{4/3}\chi^{2/3}}{g^{1/3}} \quad (29)$$

where approximate equalities have relevance to the limiting case $\kappa \to 0$.

Equations (27) and (28) then reduce to the following dimensionless equations

$$\frac{R}{L_s^{(b)}} = \xi = \sqrt{\tau} \quad \frac{d}{d\tau}\left(\tau^{3/2}\frac{d\zeta}{d\tau}\right) = \tau^{3/2} + N_\sigma\frac{\tau-\zeta^2}{\sqrt{\tau}} \quad (30)$$

in which a dimensionless criterion

$$N_\sigma = \frac{12}{11(1+a\kappa)}\frac{\sigma/\rho_l}{(CJa)^2\chi}\frac{L_t^{(b)}}{L_s^{(b)}} \approx \frac{0.963}{(CJa)^{8/3}}\frac{\sigma/\rho_l}{\chi^{4/3}g^{1/3}} \quad (31)$$

characterizes the influence caused by surface tension force.

We start by considering the simplest extreme case, when N_σ is very small and therefore the second term on the right-hand side of equation (30) essentially drops out. The wanted solution to the equation at natural initial conditions, $\zeta = d\zeta/d\tau = 0$ at $\tau = 0$, is trivial. It reads $\zeta = \tau^2/5$. The moment of bubble detachment is defined by requiring that s coincide with current bubble radius R, whence the dimensionless time of detachment $\tau_d = 5^{2/3} \approx 2.924$. The corresponding dimensional time and bubble detachment radius are

$$t_d = L_t^{(b)}\tau_d \approx 2.924L_t^{(b)} \approx 2.278(CJa)^{2/3}\chi^{1/3}g^{-2/3}$$

$$R_d = L_s^{(b)}\sqrt{\tau_d} \approx 1.710L_s^{(b)} \approx 1.570(CJa)^{4/3}\chi^{2/3}g^{-1/3} \quad (32)$$

the last approximate equalities in each formulation being valid at the limit $\kappa \to 0$.

A significant feature of equations (32) consists in that they show detachment characteristics to be essentially dependent on the thermophysical properties of the liquid. Conventional formulae for these detachment characteristics usually fail to incorporate such a dependence in principle, contrary to some experimental correlations which clearly witness its existence. For instance, bubble departure diameter has been found in refs. [15, 16] to be proportional to $Ja_*^{5/4}$, Ja_* standing for a modified Jakob number with ΔT substituted by T_s. This agrees with equations (32) even quantitatively, because the difference between the theoretical and experimental exponents of 4/3 and 5/4 is rather negligible and presumably lies within experimental error. The limiting regime considered above can conditionally be attributed to high gravity boiling. It is easy to see, however, that this regime is possible not only in normal or elevated gravity but also at an arbitrary, no matter how small, gravity level if the Jakob number is large enough. The appearance of this extreme regime is also favoured by an increase in the thermal diffusivity of the liquid and a decrease in the surface tension coefficient at the liquid–vapour interface.

Consider, next, changes in $\zeta(\tau)$, as well as in bubble detachment characteristics which are caused by variations of parameter N_σ. For definitiveness, the variations may be thought as being due to variations in σ under otherwise identical conditions. In order to come up with function $\zeta(\tau; N_\sigma)$ as a solution to equation (30), suitable initial conditions must be imposed. These conditions have to depend, of course, on the peculiarities of the nucleation site where the bubble evolves, but this poses a problem since little is generally known about these peculiarities. Since we intend to avoid this difficulty and since we also wish to leave various problems of original vapour nucleus formation and incipient boiling completely out of the picture, initial conditions have to be posited with a hypothetical macroscopic bubble in mind, rather than a vapour nucleus. Admittedly, the initial bubble is large as compared with the nucleus, and it can be described with the help of asymptotics to solutions of equation (30) which are valid at short times. The desired asymptotic representation follows from the equation itself,

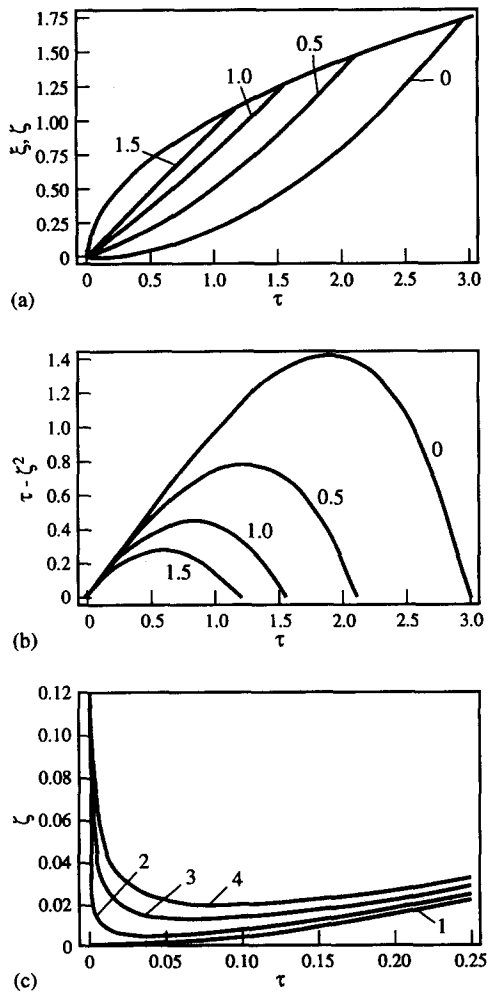

Fig. 2. Integral curves (a) and dimensionless bubble base area (b) for equation (30) at initial conditions stated at $\tau = 10^{-4}$ in accordance with equation (33) and at different N_σ (figures at the curves); the upper curve $\xi = \tau^{1/2}$ in (a) presents dimensional bubble radius; (c) illustrates the effect of initial conditions: curves 1–4 correspond to $n = 0, 0.1, 0.3$ and 0.5 in condition $\zeta\tau^{-1/2} = n$, respectively, at $N_\sigma = 0$.

$$\zeta(\tau; N_\sigma) \approx (2N_\sigma/3)\tau, \quad \tau \ll N_\sigma. \tag{33}$$

The relevant solutions to equation (30) obtained in compliance with equation (33) are illustrated by the curves in Fig. 2. All of the curves in Figs. 2(a) and (b) satisfy the initial conditions imposed at $\tau = 10^{-4}$. The curves in Fig. 2(a) intersect curve $\xi = \tau^{1/2}$, which represents the dimensionless bubble radius, where they terminate. Corresponding values τ_d give the dimensionless bubble detachment time at different N_σ, which is a decreasing function of this parameter.

Thus, total duration of bubble evolution up to the moment of detachment shortens and bubble departure size diminishes as surface tension force increases at a fixed buoyancy. This is completely understandable from the physical point of view since surface tension force adds to the action of the force due to buoyancy and so speeds up bubble detachment.

Bubble base area time dependence is illustrated in Fig. 2(b) for the same conditions as in Fig. 2(a). At first, this area increases with time due to bubble expansion and to the resulting advance of the bubble meniscus along the wall. After that, when the bubble centre rises sufficiently fast, the bubble base area begins to decrease in spite of the bubble continuing to grow, and it eventually vanishes just at the moment of bubble detachment.

Equation (33) proves the initial small bubble to be almost hemispherical, which is quite compatible with the aforementioned concept of two-stage bubble growth. If the initial bubble deviates from a hemisphere for some chance reason, it quickly resumes hemispherical form, as evidenced by the curves in Fig. 2(c). The curves show how ratio s/R changes with time at $N_\sigma = 0$ and at different initial conditions. Irrespective of its initial value, ratio s/R rapidly falls off to nearly zero, and this corresponds to the state where the bubble is a hemisphere attached to the wall. Thereupon ζ begins to grow almost in accordance with the corresponding curve of Fig. 2(a). Apart from other things, the fact that bubble evolution is insensitive to an exact form of initial conditions completely justifies using asymptotics (33) to state these initial conditions.

7.2. *Bubbles dominated by surface tension*

If surface tension force prevails in promoting bubble transformation into a full sphere, and therefore, dominates in providing its detachment, it is much more appropriate to introduce time and length scales different from those used to describe bubble motion when it is dominated by buoyancy. Such scales can be brought into action by taking into account the second term on the right-hand side of equation (28). Namely, we assume

$$t = L_t^{(\sigma)}\tau$$

$$L_t^{(\sigma)} = \left[\frac{11(1+a\kappa)}{12}\right]^2 \frac{(CJa\sqrt{\chi})^6}{(\sigma/\rho_l)^2} \approx 0.840\frac{(CJa)^6\chi^3}{(\sigma/\rho_l)^2}$$

$$s = L_s^{(\sigma)}\zeta$$

$$L_s^{(\sigma)} = \frac{11(1+a\kappa)}{12}\frac{(CJa\sqrt{\chi})^4}{\sigma/\rho_l} \approx 0.917\frac{(CJa)^4\chi^2}{\sigma/\rho_l} \tag{34}$$

the approximate equalities again implying $\kappa \ll 1$.

Equations (27) and (28) now reduce to

$$\frac{R}{L_s^{(\sigma)}} = \xi = \sqrt{\tau} \quad \frac{d}{d\tau}\left(\tau^{3/2}\frac{d\zeta}{d\tau}\right) = N_b\tau^{3/2} + \frac{\tau - \zeta^2}{\sqrt{\tau}} \tag{35}$$

with a new dimensionless parameter

$$N_b = \frac{16}{11}\frac{1-\kappa}{1+a\kappa}\frac{L_t^{(\sigma)^2}}{L_s^{(\sigma)}}g \approx 1.120(CJa)^8\frac{\chi^4 g}{(\sigma/\rho_l)^3} \tag{36}$$

characterizing the relative role played by buoyancy.

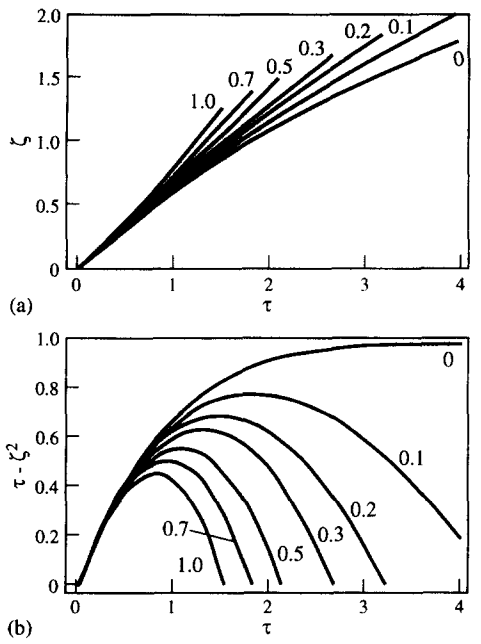

Fig. 3. Integral curves (a) and dimensionless bubble base area (b) for equation (35) at initial conditions stated at $\tau = 10^{-4}$ in accordance with equation (37) at different N_b (figures at the curves); curve $\xi = \tau^{1/2}$ is not plotted.

Since the scales identified in equation (34) are independent of gravity acceleration, it is appropriate to apply equation (35) to the boiling of a given liquid under preassigned thermal and pressure conditions, but in variable gravity, irrespective of the ratio of surface tension force to buoyancy.

The asymptotics to be employed while formulating initial conditions for solutions to equation (35) resemble those in equation (33) but are independent of parameter N_b,

$$\zeta(\tau; N_b) \approx (2/3)\tau \quad \tau \ll N_b^{-1}. \tag{37}$$

Integral curves for equation (35) that satisfy initial conditions (37) imposed at $\tau = 10^{-4}$ are plotted in Fig. 3(a), and corresponding curves for the dimensionless bubble base area are plotted in Fig. 3(b). Each of the curves in Fig. 3(a), except for the one corresponding to $N_b = 0$, terminates at a point of intersection with curve $\xi = \tau^{1/2}$. Coordinates of the termination point again determine both the whole duration of bubble evolution and the bubble departure radius. Both the duration of bubble evolution and the departure radius are monotonously decreasing functions of parameter N_b. They go to zero as N_b tends to infinity and increase limitlessly as this parameter reaches zero. It is easy to see that adding some amount of buoyancy to the surface tension force quickens the process of bubble development, in the same way, and precisely for the same reason, as adding surface tension to buoyancy does. It is worth noting that the curves in Figs. 2 and 3 contain identical physical information which is presented in terms of different variables.

A striking feature of vapour bubble evolution dominated by surface tension force is the very strong dependence of inherent time and length scales on physical properties of the liquid. Equally striking is the strong dependence of these scales on coefficient C which characterizes bubble growth and on wall temperature, as shown in equation (34). Hence, it is quite natural to anticipate that a seemingly insignificant variation of ΔT, when all other conditions are held equal, will considerably affect the main characteristics of bubble growth and detachment. This may easily be the reason for the embarrassing scatter of results in experiments carried out under apparently identical conditions, with obvious implications for evaluating and correlating experimental data. It also proves that the heat conductivity of the wall material, which is capable of affecting the local wall temperature underneath the bubble to quite a considerable degree, is of paramount significance in establishing an actual regime of bubble evolution, and consequently, of nucleate pool boiling.

If buoyancy completely disappears ($N_\sigma = 0$), as happens in complete weightlessness, only surface tension remains to provide for transformation of the bubble into a sphere. It can be readily proven, however, that surface tension force alone is insufficient to ensure bubble detachment. This is due to the surface tension force becoming progressively weaker as bubble size increases at a constant bubble base, or as the base shrinks at a fixed bubble volume. For this reason, when on the verge of detachment, the bubble base retraction that accompanies the rise of the bubble centre due to surface tension force cannot ultimately overcome the bubble base broadening that results from advance of the bubble meniscus along the wall that is due to bubble growth. As a consequence, the bubble centre continues to rise in such a way that its vertical coordinate never reaches the current bubble radius, and the required necessary condition of bubble detachment is never achieved.

This means, first of all, that the corresponding curve $\zeta(\tau)$ [the curve marked by zero in Fig. 3(a)] lies below curve $\xi = \tau^{1/2}$ for all time values, and the bubble base area monotonously increases with time to infinity, with ratio s/R tending to a constant limit, as is shown in Fig. 4. This notwithstanding, adding some amount of buoyancy, if apparently quite negligible, results in a drastic change of bubble behaviour. No matter how low gravity may be, there inevitably comes a moment at which the bubble base area ceases to increase and henceforth begins to fall off to zero, as illustrated in Fig. 4. This is because buoyancy is proportional not only to gravity acceleration but also the bubble volume. As the bubble grows, buoyancy in due course becomes strong enough to make the bubble detach itself at an arbitrarily small but finite gravity acceleration. Because of the complicated dependence of the surface tension force on the size and geometrical characteristics of the bubble attached to the wall, base area time dependence displays two maxima and a minimum during the intermediate stage of bubble

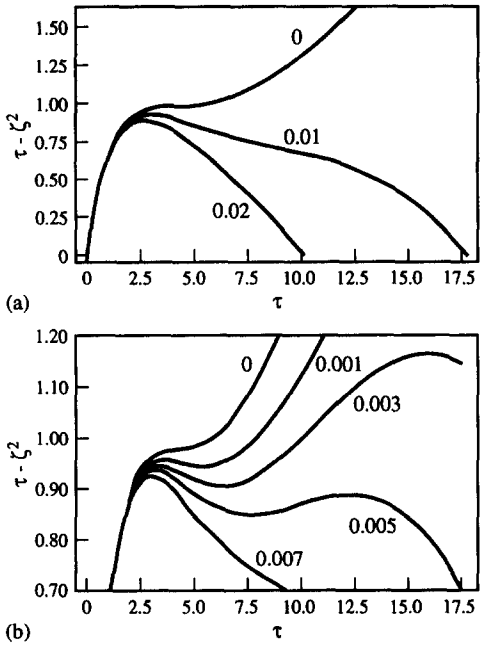

Fig. 4. Time dependence for bubble base area in low gravity; figures at the curves give N_b.

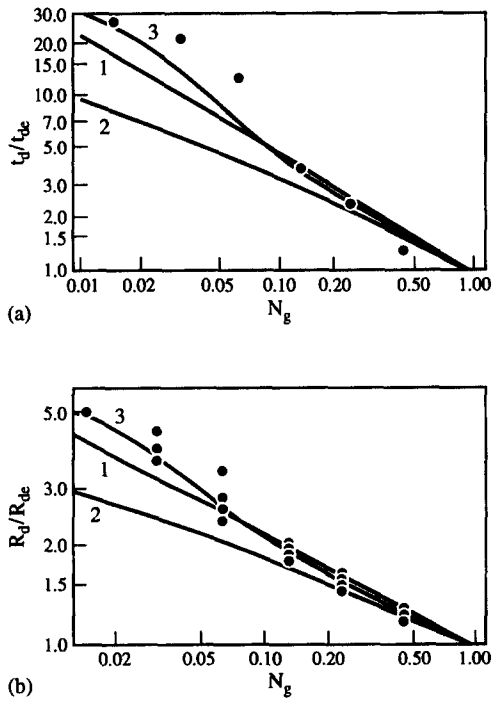

Fig. 5. Relative duration of the whole period of bubble evolution (a) and relative bubble radius at detachment (b) in reduced gravity; 1–3—theoretical curves at $N_b = \infty$ (or 0), 10 and 5×10^{-4}, respectively, dots—experimental data in refs. [2, 3].

evolution in sufficiently low gravity, as shown in Fig. 4(b). The duration of the whole evolutionary process up to detachment rapidly increases as N_b diminishes within a region of its small values. It should be stressed that the same behaviour is expected with regard to vapour bubbles developing in moderately reduced gravity, and even in normal gravity whenever parameter N_b identified by equation (36) happens to be small for any other reason (for example, an essential diminution of this parameter can be rendered by a comparatively small decrease in wall overheat ΔT).

7.3. *Influence of gravity on bubble detachment characteristics*

In order to compare theoretical expectations with experimental evidence, we shall consider the influence caused by gravity on bubble evolution duration and on bubble detachment radius. A ratio relating the whole time of bubble evolution at a few levels of reduced gravity to the analogous time in Earth gravity, and also a similar ratio for the bubble departure diameter, have been determined in some experiments that were conducted on the boiling of saturated water under normal pressure conditions [2, 3]. These ratios are illustrated by dots in Fig. 5. In this figure, the data on evolution time and on departure diameter have been taken from the curves in Figs. 16 and 19 of ref. [3], respectively. In view of equation (32), the theoretical evaluation results in formulae

$$\frac{t_d}{t_{de}} = \frac{\tau_d}{\tau_{de}} N_g^{-2/3} \quad \frac{R_d}{R_{de}} = \left(\frac{\tau_d}{\tau_{de}}\right)^{1/2} N_g^{-1/3} \quad N_g = \frac{g}{g_e} \tag{38}$$

where τ_d and τ_{de} are understood as functions of parameter N_σ at corresponding gravity.

It follows at once that in the limiting case of very high gravity, that is, when $N_\sigma \approx 0$ and when both aforementioned dimensionless time values approximately equal 2.924, t_d and R_d will increase with gravity reduction. These quantities are really proportional to $g^{-2/3}$ and $g^{-1/3}$ (but not to $g^{-1/2}$ as suggested in ref. [3]), respectively. These power laws are illustrated in Fig. 5 by the curves marked with 1.

A simple evaluation suffices to show that bubble dynamics are governed, given conditions described in the experiments conducted in refs. [2, 3], by surface tension force, rather than by buoyancy. Because of this, we prefer to make use of the variables identified in equation (34). Since the scales in equation (34) do not involve gravity acceleration, the ratios under question have to be reformulated as

$$\frac{t_d}{t_{de}} = \frac{\tau_d}{\tau_{de}} \quad \frac{R_d}{R_{de}} = \left(\frac{\tau_d}{\tau_{de}}\right)^{1/2} \tag{39}$$

with τ_d and τ_{de} now being understood as functions of parameter N_b as specified in equation (36).

As N_{be} decreases from infinity, the theoretical curves in Fig. 5 decline and reach their lowest point at approximately $N_{be} \approx 10$ (curves 2 in Fig. 5). Thereupon the curves begin to ascend as N_{be} continues to fall below 10. They come to the position marked 3 at $N_{be} = 5 \times 10^{-3}$. However, when N_{be} continues on to

zero, the curves in Fig. 5 again tend to the curves marked with 1.

Allowing for some uncertainties in experimental conditions that may be inherent in refs. [2, 3], we can deduce from these experimental conditions that the relevant value of N_{be} lies somewhere between 10^{-4} and 10^{-3}, so that the curves 3 in Fig. 5 may be looked upon as approximate theoretical evaluations of the quantities identified in equation (39). The agreement between experimental and theoretical results in Fig. 5 is good.

8. EFFECT OF EVAPORATION FROM THE MICROLAYER

Within the framework of the simplified model presented thus far, bubble radius changes with time in accordance with the parabolic law in equation (30) or (35), irrespective of an actual ratio of buoyancy to surface tension force. Consequently, the coefficient in this law appears to be independent of both gravity and surface tension. This seeming independence is a direct result of neglecting vaporization at the free microlayer surface when deriving the growth law.

The total amount of vapour emerging from the free microlayer surface is proportional to the area of this surface. Since surface area depends on bubble centre motion as it is conditioned by the action of all relevant forces, factors determining these forces must influence the area, and hence, bubble growth rate as well. Thus one may foresee that allowance for evaporation from the microlayer will result in a slight dependence of the growth rate on all the parameters specifying these forces. In order to investigate such relatively subtle effects, we need to first of all turn from the parabolic law to original equation (27) that describes thermally controlled bubble growth.

By using the scales identified in equation (34) when dealing with equations (27) and (28), we arrive at a set of two nonlinear dimensionless equations,

$$\frac{d\xi}{d\tau}=\frac{1}{2\sqrt{\tau}}\left[1+\left(N_m-\frac{1}{2}\right)\frac{\xi-\zeta}{\xi}\right]$$

$$\frac{d}{d\tau}\left(\xi^3\frac{d\zeta}{d\tau}\right)=N_b\xi^3+\frac{\xi^2-\zeta^2}{\xi} \qquad (40)$$

instead of equations (35). Initial conditions are now to be stated with the help of asymptotics

$$\xi\approx(N_m+0.5)\sqrt{\tau}\quad \zeta\approx(2/3)(N_m+0.5)^{-2}\tau\quad \tau\ll N_b^{-1} \qquad (41)$$

which substitute for those in equation (37).

Typical solutions of problem (40), (41) are presented in Fig. 6. As N_m increases over 1/2 at a fixed N_b, the process of bubble development becomes more and more lengthy, with a corresponding enlargement of bubble volume at detachment [Fig. 6(a)]. This is indicative of a general effect on bubble development

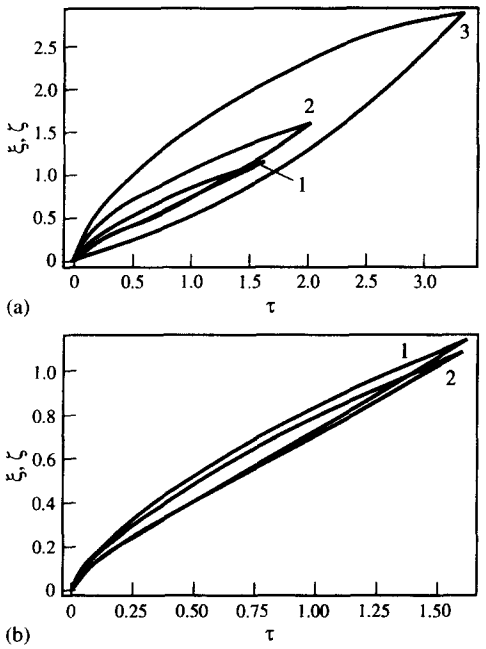

Fig. 6. Influence of evaporation from microlayer on bubble dynamics at $N_m = 0.5$ (curves marked with 1) and $N_m = 1.5$, 2.5 (curves 2 and 3 in a) and $N_m = 0$ (curve 2 in b).

duration that may be the result of an augmentation in bubble growth rate. Actually, since the bubble base expands along the wall as the bubble grows without changing its shape, the bubble centre has to move upwards for a larger distance in order to make the bubble area go to zero. Further, the lower the Prandtl number, the larger the parameter N_m. Thus, the general effect of evaporation from the microlayer on bubble development duration is especially pronounced in the boiling of liquid metals. It is worthwhile to as well note that N_m grows as C decreases, which condition is specific to the boiling of subcooled liquids. We must be careful, however, when drawing conclusions about the boiling of subcooled liquids because parameter C also bears upon the definition of relevant scales specified in equation (29). If N_m is smaller than 1/2, as may be characteristic for liquids with $Pr \geqslant 1$ at $C \geqslant 1$, then bubble growth rate is insignificantly affected by the corrective term on the right-hand side of the first equation (40) (this corrective term is due both to evaporation from the microlayer and to the change in evaporation from the bulk of the surrounding liquid; this change in evaporation from the bulk is caused by the fact that bubble shape deviates from that of a sphere). This is evidenced by Fig. 6(b).

As already demonstrated, if evaporation from the microlayer is taken into account in the dynamic equation describing bubble growth, it is natural to expect that bubble growth rate is dependent on parameters that determine the forces acting on the bubble. Such an expectation is fully confirmed by curves in Fig. 7. The curves show, first of all, that the actual growth law differs from the parabolic law. In the second place,

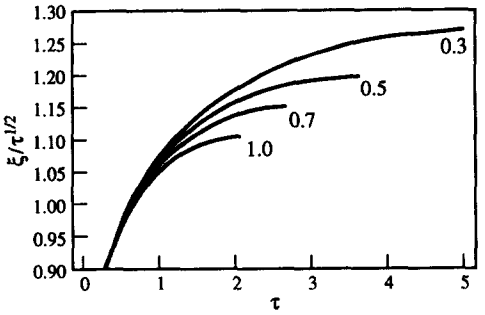

Fig. 7. Quantity $\xi\tau^{-1/2}$ characterizing deviation of actual bubble growth law from parabolic law due to evaporation from microlayer at $N_m = 1.5$ and $N_b = 0.3$, 0.5, 0.7 and 1 (figures at the curves).

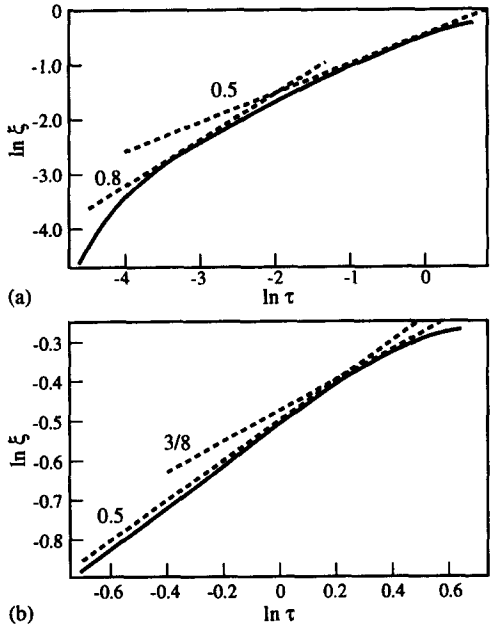

Fig. 8. Bubble growth at negligible evaporation from the bulk and at negligible surface tension (explanation in the text).

the growth rate is higher, the smaller the parameter N_b, or the lower the gravity, as long as surface tension is kept invariable. A similar conclusion can be demonstrated true when the gravity level is fixed: growth rate increases when surface tension force is diminished. In both these cases, increased growth rate is attributable to the fact that a decrease in the total force favouring bubble departure from the wall slows down the transformation of the bubble into a full sphere, and thereby, results in a certain relative enlargement of the bubble base area at any given particular moment. The increase in the bubble base area enables an additional amount of vapour at the lower bubble surface to be produced, and consequently, causes the bubble growth rate to increase.

On the contrary, when $N_m - 1/2$ is negative, and there is a reduction of gravity at an invariable surface tension or vice versa, there is a decrease in growth rate due to the bubble not reaching a fully spherical shape. In this case, increased vaporization from the microlayer does not compensate for a corresponding reduction of vaporization from the bulk. A reduced vaporization from the bulk results from a decrease in the area of the upper spherical part of the bubble surface as compared with the overall surface area of a sphere with the same volume. However, such a growth rate decrease in negligible, and does not deserve our further attention.

By way of example, Fig. 8 shows a theoretical curve that follows from equations (40) and (41) in a simplified case where (1) evaporation from the bulk is entirely neglected as compared with evaporation from the microlayer and (2) surface tension force is neglected as compared with buoyancy. This curve describes bubble growth from a hemispherical cavity with $\xi_0 = 0.01$ and $\zeta_0 = (d\zeta/d\tau)_0 = 0$ at $\tau_0 = 0.01$. This curve proves the parabolic law to hold approximately true for a lengthy intermediate stage of bubble growth, and this stage constitutes the main portion of the whole growth period. However, bubble size increases in a short initial stage faster than required by that law. Moreover, the parabolic law does not hold strictly true for the final finite stage of bubble growth where bubble growth supposedly slows down due to a progressive decrease in the evaporation surface immediately before detachment.

It is rather telling that the curves in Fig. 7 strikingly resemble the experimental curves obtained in refs. [2, 3]. The cited papers have also demonstrated that bubble radius grows faster in an initial period than this is required by the parabolic law, with the time exponent ranging from 0.5 to 0.8 for particular bubbles. At the same time, these papers show that the radius grows slower than required by the parabolic law in a certain final stage of growth where the time exponent was found to be approximately 3/8. These power laws are illustrated in terms of logarithmic variables in Fig. 8, together with the parabolic law characteristic of the most prolonged intermediate stage of growth.

9. CONCLUDING REMARKS

The main achievement of the present work consists in our having succeeded in rigorously deriving expressions for the forces that condition vapour bubble formation at nucleation sites located on a superheated wall under nucleate pool boiling conditions. Our model leads to the essentially important and novel conclusion that surface tension effects bring about an effective force that facilitates bubble detachment, but that this force by no means keeps the bubble pressed to the wall, as was postulated without sufficient foundation in practically all preceding theoretical papers on this subject. It can be readily proven that this conclusion regarding the capacity of the surface tension force to facilitate bubble detachment is by no means abetted by the assumptions that have been made in this paper in order to simplify calculations.

It is just this conclusion that calls into question other theoretical papers on vapour bubble growth and detachment published to date, and that enables us to anticipate that the present paper should have a great impact on future studies of vapour bubble dynamics and of boiling heat transfer in general.

In particular, this conclusion helps us to understand two so far unexplained phenomena: (1) the complicated character of the dependence of bubble detachment characteristics not only on factors that determine forces acting on the bubble, but also on physical properties of the liquid and its vapour, and also (2) the very fact of the dependence of the bubble growth rate on the aforementioned force factors. Fortunately enough, the latter dependence is rather slight, and the conventional formulae for bubble growth rate may be used without inducing an appreciable error. However, the conventional formulae for bubble detachment characteristics which are founded on the substantially incorrect premise that surface tension force impedes bubble detachment are intrinsically flawed, and for this reason, must be revised.

In conclusion, we wish to point out that the lack of space has prevented us from listing a great many numerical calculation results that were actually performed over a wide range of relevant parameters. On the whole, research opportunities afforded by our novel formulation of dynamic equations for vapour bubbles are by no means exhausted by the contents of the present paper.

Acknowledgement—This study was performed while Prof. Yuri Buyevich held a National Research Council Research Associateship at the NASA Ames Research Center.

REFERENCES

1. B. Mikic, W. M. Rohsenow and P. Griffith, On bubble growth rates, *Int. J. Heat Mass Transfer* **13,** 657–666 (1970).
2. R. Siegel and E. G. Keshock, Effects of reduced gravity on nucleate boiling bubble dynamics in saturated water, *A.I.Ch.E. Jl* **10,** 509–515 (1964).
3. R. Siegel, Effects of reduced gravity on heat transfer. In *Advances in Heat Transfer*, Vol. 4, pp. 143–228. Academic Press, New York (1967).
4. H. Merte, Jr, Nucleate pool boiling in variable gravity. In *Low-Gravity Fluid Dynamics and Transport Phenomena*, pp. 15–69. American Institute Aeronautics Astronautics, Washington, D.C. (1990).
5. J. Straub, M. Zell and B. Vogel, Pool boiling in a reduced gravity field, *Proceedings of Heat Transfer 1990, Ninth International Heat Transfer Conference*, Jerusalem, Vol. 1, pp. 91–112 (1990).
6. R. Mei, W. Chen and J. F. Klausner, Vapor bubble growth in heterogeneous boiling, *Int. J. Heat Mass Transfer* **38,** 909–934 (1995).
7. M. Akiyama, F. Tachibana and N. Ogawa, Effect of pressure on bubble growth in pool boiling, *Bull. JSME* **12,** 1121–1128 (1969).
8. N. S. Srinivas and R. Kumar, Prediction of bubble growth rates and departure volumes in nucleate boiling at isolated sites, *Int. J. Heat Mass Transfer* **27,** 1403–1409 (1984).
9. M. G. Cooper, The microlayer and bubble growth in nucleate pool boiling, *Int. J. Heat Mass Transfer* **12,** 915–933 (1969).
10. S. J. D. Van Stralen, M. S. Sohal, R. Cole and W. M. Sluyter, Bubble growth rates in pure and binary systems: combined effect of relaxation and evaporation microlayers, *Int. J. Heat Mass Transfer* **18,** 453–467 (1975).
11. L. D. Koffman and M. S. Plesset, Experimental observations of the microlayer evaporation during bubble growth on a heated solid, *Trans. ASME, J. Heat Transfer* **105,** 625–632 (1983).
12. Zh. Guo and M. S. El-Genk, Liquid microlayer evaporation during nucleate pool boiling on the surface of a flat composite wall, *Int. J. Heat Mass Transfer* **37,** 1641–1655 (1994).
13. Y. S. Kao and D. B. R. Kenning, Thermocapillary motion near a hemispherical bubble on a heated wall. *J. Fluid Mech.* **53,** 715–735 (1972).
14. Y. Abe, T. Oka, Y. H. Mori and A. A. Nagashima, Pool boiling of a non-azeotropic binary mixture under microgravity, *Int. J. Heat Mass Transfer* **37,** 2405–2413 (1994).
15. Cole and W. M. Rohsenow, Correlation of bubble departure diameters for boiling of saturated liquids, *Chem. Engng Progr. Symp. Ser. A.I.Ch.E.* **65,** 211–213 (1969).
16. W. M. Rohsenow, Boiling. In *Handbook of Heat Transfer Fundamentals*, pp. 12-1–12-94. McGraw-Hill, New York (1985).
17. T. H. Cohran and J. Aydelott, The effect of subcooling and gravity level on boiling in the discrete bubble regime. NASA Technical Note TN D-3449 (1966).
18. Yu. A. Buyevich and V. N. Mankevich, Interaction of dilute mist flow with a hot body, *Int. J. Heat Mass Transfer* **38,** 731–744 (1995).
19. J. F. Davidson and B. O. G. Schüler, Bubble formation at an orifice in an inviscid liquid, *Trans. Instn Chem. Engrs* **38,** 335–342 (1960).
20. C. P. Witze, V. E. Schrook and P. L. Chambre, Flow about a growing sphere in contact with a plane, *Int. J. Heat Mass Transfer* **11,** 1637–1646 (1968).
21. S. Goldstein, *Modern Developments in Fluid Dynamics*. Oxford University Press, Oxford (1938).
22. L. Z. Zeng, J. F. Klausner and R. Mei, A unified model for the prediction of bubble detachment diameters in boiling systems, *Int. J. Heat Mass Transfer* **36,** 2261–2279 (1993).
23. Yu. A. Buyevich and V. A. Ustinov, Hydrodynamic conditions of transfer processes through a radial jet spreading over a flat surface, *Int. J. Heat Mass Transfer* **37,** 165–173 (1994).
24. A. E. Wraith, Two stage bubble growth at a submerged plate orifice, *Chem. Engng Sci.* **26,** 1659–1671 (1971).